Two-dimensional phonon hydrodynamics in narrow strips

A. Sellitto* and I. Carlomagno†

Department of Mathematics, Computer Science and Economics,

University of Basilicata, Campus Macchia Romana, 85100, Potenza, Italy

D. Jou‡

Department of Physics, Autonomous University of Barcelona,

08193 Bellaterra, Catalonia, Spain and

Institut d'Estudis Catalans, Carme 47, Barcelona 08001, Catalonia, Spain

(Dated: May 16, 2022)

Abstract

Heat flow along two-dimensional strips as a function of the Knudsen number is examined in two different versions of heat-transport equations with non-local terms, with or without heat slip flow. In both of them, a parabolic heat profile corresponding to the Poiseuille phonon flow may appear in some domains of temperature, or of the Knudsen number, in the transition from the Fourier regime to the ballistic one. The influence of the slip heat flow on such transition is discussed.

PACS numbers: 63.22.Kn,65.80.-g,63.22.-m,44.10.+i

Keywords: phonon hydrodynamics, ballistic regime, diffusive regime, effective thermal conductivity, two-dimensional nanosystems

*Electronic address: ant.sellitto@gmail.com

†Electronic address: isabellacarlomagno85@gmail.com

‡Electronic address: david.jou@uab.cat

I. INTRODUCTION

Material systems with characteristic sizes of the order of nanometers exhibit interesting optical, magnetic, electrical, and/or photoelectrical properties. In the last years several research groups are intensifying their attention on the contribution of collective hydrodynamic-like phonon behavior on two-dimensional (2D) nanosystems [9, 14, 15, 30]. Silicon nanolayers, boron nitride nanolayers [2, 5, 40], and graphene [3, 4, 18] have especially attracted the attention. In particular, it has been recently argued that in suspended graphene [30] and other 2D systems [9] Poiseuille phonon flow could be observed at higher temperatures and in wider temperature ranges than in three-dimensional (3D) systems, because in 2D systems the normal (momentum conserving) phonon-phonon collisions are two orders of magnitude higher than those in 3D systems. Thus, analysis of this regime in 2D situations has become a topic of current interest.

Phonons, which are the main heat carriers in non-metallic nanosystems, can undergo not only a diffusive regime, but also a hydrodynamic regime (Poiseuille-like) and a ballistic one. In the first case, the heat transfer can be described by means of the Fourier law. In the latter cases, instead, Fourier law breaks down [11, 12, 26, 28, 30, 38, 41, 46], and more general constitutive equations for the local heat flux are needed [13, 27].

Different theories and/or approaches can be found in literature to face with the breakdown of Fourier law at nanoscale and to describe thermal transport in nanosystems [7, 11, 14, 22, 29, 37, 39, 42, 46]. Here we focus our attention on phonon hydrodynamics [1, 26, 30], since it connects mesoscopic and microscopic approaches.

It seems worth noticing that the term *phonon hydrodynamics* may be interpreted in two different ways:

a) as a particular regime of phonon flow wherein normal phonon collisions and collective effects are dominant thus leading to a Poiseuille-like flow,

b) as a more general thermodynamic model of heat transfer, wherein non-local effects play a relevant role [1, 16, 23, 24, 26, 33–35, 45] in such a way that, for very small systems, the form of the constitutive equation for the local heat flux is analogous to that for the velocity of a viscous fluid in classical hydrodynamic.

The usual starting point of phonon hydrodynamics (in the second meaning) is the so-

called Guyer-Krumhansl equation [23, 24], which is characterized by the inclusion of second-order non-local effects in the evolution equation for the heat flux. One version of that equation is

$$\tau_R \dot{\mathbf{q}} + \mathbf{q} = -\lambda \nabla T + a^2(T)\, \ell^2 \left(\nabla^2 \mathbf{q} + 2 \nabla \nabla \cdot \mathbf{q} \right), \tag{1}$$

wherein τ_R is the relaxation time related to resistive (i.e., momentum non-conserving) collisions between phonons, T the temperature, λ the usual Ziman limit for the bulk thermal conductivity [47], ℓ an average phonon mean-free path, and $a(T)$ means a dimensionless scalar function [8].

In the hydrodynamic regime (i.e., when in Eq. (1) the contribution of the heat flux may be neglected with respect to its spatial derivatives [1, 34, 35]), the phonons exhibit a macroscopic drift motion [30] which is the main difference between that regime and the more well-known diffusive and ballistic regimes. Due to that drift motion, in phonon-hydrodynamic regime the heat-flux profile is not uniform everywhere and may exhibit a parabolic profile analogous to that of Poiseuille hydrodynamic flow.

In steady states, in Refs. [1, 34, 35] Eq. (1) has been used to describe the size-dependency of the effective thermal conductivity in nanosystems of different sizes and shapes. In doing that, it was assumed that the local heat flux is the sum of two different contributions: the bulk contribution $\mathbf{q}_\mathrm{b}$, arising from the solution of Eq. (1) with vanishing boundary conditions, and a wall contribution $\mathbf{q}_\mathrm{w}$, which may be related to $\mathbf{q}_\mathrm{b}$ by a constitutive equation of the form

$$\mathbf{q}_\mathrm{w} = Ca\ell \left. \frac{\partial \mathbf{q}_\mathrm{b}}{\partial \xi} \right|_\gamma, \tag{2}$$

up to the first order in ℓ [8]. In Eq. (2) ξ means the normal direction to the wall cross section (pointing towards the flow), and γ is the curve accounting for the outer surface of the transversal section of the system. Moreover, C is a positive constant related to the properties of the walls, namely, to the combination of diffusive and specular phonon-wall scattering [1, 10, 19, 35, 36] as

$$C = 2 \left(\frac{1+p}{1-p} \right)$$

with p being the relative number of phonon-wall specular collisions as compared to the total number of specular and diffusive collisions. This is well-known for gases and for electron

collisions [47] and it can be also adopted for the phonons [8]. Since p may only vary in the range $[0;1]$, the parameter C should be larger than 2. Small values of C mean that diffusive phonon-wall collisions are predominant over specular ones. Conversely, large values of C mean that the specular phonon-wall scattering dominates over the diffusive one. The relation between the parameters a, C and ℓ in the boundary condition (2) has been investigated in Ref. [8]. In Refs. [1, 34, 35] Eqs. (1) and (2) were used to provide a phenomenological way to explicitly describe the effects of phonon-wall collisions [2, 31, 32] through a formalism which is parallel to that of rarefied fluid dynamics [10, 19, 36].

In principle, the wall contribution $\mathbf{q}_{\rm w}$ is restricted to a thin region near the walls, the so-called Knudsen layer, whose thickness is of the order of mean-free path of the heat carriers. Far from the walls, $\mathbf{q}_{\rm w}$ is vanishingly small [1, 34, 35]. The use of Eq. (2) allows to account for the boundary scattering, which is the main cause of the non-uniform heat-flux profile in the hydrodynamic regime. We note that from the theoretical point of view, the approach used in Refs. [1, 34, 35] prescribes that only the bulk contribution $\mathbf{q}_{\rm b}$ is considered as a state-space variable.

An alternative way to account for the boundary scattering by means of a slip heat flux is to assume that the local heat flux $\mathbf{q}$, instead of $\mathbf{q}_{\rm b}$, is the solution of Eq. (1) together with the following Robin-type boundary condition

$$\mathbf{q}|_{\gamma} = Ca\ell \left.\frac{\partial \mathbf{q}}{\partial \xi}\right|_{\gamma} . \tag{3}$$

In this way, one can assume that $\mathbf{q}$ (and not its partial contribution $\mathbf{q}_{\rm b}$) belongs to the state spaces as it is usual in Extended Thermodynamics [12, 26, 28]. In the present paper we principally investigate the alternative way above.

As a brief summary, we say that the paper runs as follows.

In Sec. II we use Eq. (1), complemented with Eq. (3), to show how phonon hydrodynamics may be used to investigate heat transfer in 2D narrow strips in a wide temperature range (or Knudsen-number range). Therein we also derive the effective thermal conductivity and compare the theoretical expression with that obtained in Refs. [1, 35].

In Sec. III we derive the theoretical behavior both of the local heat flux, and of the effective thermal conductivity by means of an approach closer to the original proposal by Guyer and Krumhansl [23, 24], which directly introduces the phonon-wall interactions in the differential equation (1) and assumes $\mathbf{q} = \mathbf{0}$ on the walls. In other words, in this section we

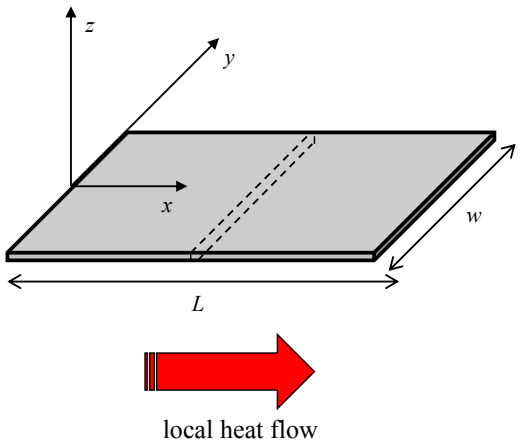

FIG. 1: Sketch of a 2D strip (or a very thin layer). The height of that system (i.e., the characteristic size along the z axis) is very small and negligible with respect to its length L and width w (that is, the characteristic sizes along the x and y axes, respectively). The arrow stands for the direction of the local heat flux along the x axis. By means of a dashed line, in figure we also indicate a generic cross section yz which, in the case of 2D strip, reduces to a line along the y axis. In figure x spans in $[0; L]$, and y spans $[-w/2; w/2]$.

assume that in Eq. (1) λ is a size-dependent resistive thermal conductivity, and the quantity $a\ell$ in the non-local term is related to normal phonon-phonon collisions, the dynamical role of which has been recently stressed out in a microscopic kinetic-collective model of heat transport in Refs. [14, 15].

In Sec. IV the main results are finally summarized.

II. PHONON HYDRODYNAMICS IN 2D NARROW STRIPS

In the present section we apply Eqs. (1) and (3) to study the thermal transport in a 2D strip (or a very thin layer). In particular, we assume that the thickness of the layer is much smaller than its other two characteristic sizes. This is the case, for example, of graphene, which is a flat monolayer of carbon atoms tightly packed into a 2D honeycomb lattice [18]. For the sake of illustration, in Fig. 1 a sketch of the system we are analyzing in the present paper can be seen. Therein the dashed lines indicate a generical cross section yz which, in the case of 2D nanosystems, reduces to a line along the y axis.

In particular we assume steady states in such a way that, from the local balance of internal

energy per unit volume u in the absence of heat source, namely,

$$\dot{u} + \nabla \cdot \mathbf{q} = 0, \tag{4}$$

with $\dot{u}$ being the material time derivative of u, one has $\nabla \cdot \mathbf{q} = 0$ and, consequently, Eq. (1) reduces to

$$\mathbf{q} = -\lambda \nabla T + a^2 (T)\, \ell^2 \nabla^2 \mathbf{q}. \tag{5}$$

If we assume that $\mathbf{q}$ may only flow along the x axis, and that the temperature gradient is constant along the layer, the general solution of Eq. (5) is

$$q (y) = \lambda \frac{\Delta T}{L} + A \exp\left(\frac{y}{\ell}\right) + B \left(-\frac{y}{\ell}\right), \tag{6}$$

wherein $\Delta T/L = -\nabla T$, and A and B are two arbitrary integration constants. Moreover, in this case the boundary condition (3) becomes

$$q\left(\frac{w}{2}\right) = -C_1 \ell \left.\frac{\partial q}{\partial y}\right|_{y=w/2}, \tag{7}$$

wherein $C_1 \equiv a (T)\, C$, and w is the width of the strip in such a way that $-w/2 \leq y \leq w/2$. For symmetry reasons, if we use the further boundary condition

$$\left.\frac{\partial q}{\partial y}\right|_{y=0} = 0, \tag{8}$$

which ensures that the heat-flux profile attains an extremum in the center line of the strip (in any yz plane), then the coupling of Eqs. (6)–(8) yields

$$q (y) = \lambda \left\{ 1 - \left[\frac{1}{1 + C_1 \tanh\left(\frac{1}{2\,\mathrm{Kn}}\right)} \right] \frac{\cosh\left(\frac{y}{\ell}\right)}{\cosh\left(\frac{1}{2\,\mathrm{Kn}}\right)} \right\} \frac{\Delta T}{L}, \tag{9}$$

wherein $\mathrm{Kn} = \ell/w$ is the Knudsen number.

A. Results for the local heat-flux profile

In Fig. 2 we plot the behavior of the nondimensional heat flux $q_* = q/(\lambda \Delta T/L)$ for different values of the Knudsen number (namely, $\mathrm{Kn} = 0.01$ corresponding to the line with the right-pointing triangle markers, $\mathrm{Kn} = 0.1$ corresponding to the line with the square markers, $\mathrm{Kn} = 0.5$ corresponding to the line with the circle markers, $\mathrm{Kn} = 1$ corresponding

to the line with the upward-pointing triangle markers, and Kn = 10 corresponding to the line with plus-sign markers), and for different values of the nondimensional product $C_1 \equiv a\,(T)\,C$ (i.e., $C_1 = 0.05$, $C_1 = 0.5$, $C_1 = 2$ and $C_1 = 10$). The results in that figure have been obtained from Eq. (9).

In the vertical axis of each subfigure the dimensionless quantity $y_* \equiv y/w$ spans in the range $[-0.5; 0.5]$. In other words, the total width of the strip is taken as the reference length with respect to which the other lengths are referred to. This allows that changes in Kn may be due to changes in w at a constant ℓ, or to changes in ℓ at a constant w. Since the phonon mean-free path ℓ depends on temperature (in general, the smaller T, the larger ℓ), we may therefore equivalently claim that q_* in Fig. 2 is plotted as a function of the average temperature of the system, for a given w. Thus, the approach based on Eqs. (1)-(3) also allows us to investigate the behavior of the heat flux in a wide temperature range.

Depending on Kn, the different characteristic behaviors of the local heat flux can be seen in Fig. 2. Their main features are commented below.

1. *Law values of* Kn *(Fourier diffusive regime)*

When the Knudsen number is small, the regime of heat transfer is diffusive. As it can be seen from Fig. 2, in such a case (see, for example, the curves corresponding to Kn = 0.01) the heat-flux profile has a shape which is almost uniform across the strip, whatever the values of C_1 is. In particular, if Kn $\to$ 0, then the heat-flux profile tends to the following (diffusive) limit behavior

$$q_{\text{diff,lim}} = \lambda \frac{\Delta T}{L}. \tag{10}$$

The uniform profile, which is that predicted by the classical Fourier law, characterizes the diffusive regime. In diffusive regime the phonons undergo multiple scattering inside the strip, since their mean-free path is much smaller than the characteristic size, but they do not have a macroscopic drift motion [30]. The heat-flux profile is uniform because the umklapp phonon-phonon collisions, as well as the phonon-impurity and the phonon-defect collisions (which are felt everywhere in the bulk of the system) are prevalent over the phonon-boundary scattering (which, instead, mainly occurs near the boundary of the system, that is, in the so called Knudsen layer [1, 35]).

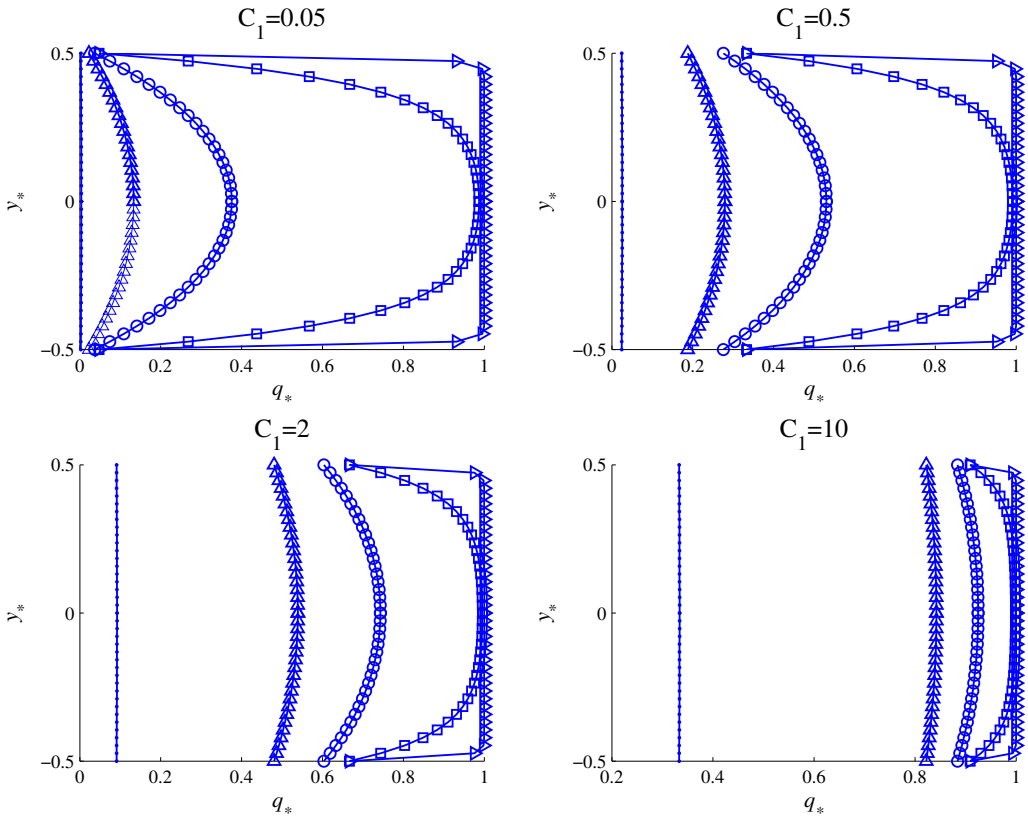

FIG. 2: Profile of the nondimensional heat flux $q_* = q/\left(\Delta T/L\right)$ across the strip for different values of the Knudsen number (Kn $= 0.01$ corresponding to the line with the right-pointing triangle markers, Kn $= 0.1$ corresponding to the line with the square markers, Kn $= 0.5$ corresponding to the line with the circle markers, Kn $= 1$ corresponding to the line with the upward-pointing triangle markers, and Kn $= 10$ corresponding to the line with plus-sign markers), and of the nondimensional product $C_1 \equiv a\left(T\right)C$ (i.e., $C_1 = 0.05$, $C_1 = 0.5$, $C_1 = 2$ and $C_1 = 10$). The results arise from Eq. (9). In each subfigure the dimensionless variable $y_* = y/w$ on the vertical axis spans in the range $[-0.5; 0.5]$.

We explicitly note that for law values of Kn, from Fig. 2 it is possible to see a slight discrepancy between the results predicted by Eq. (9) and those arising from the strict use of a Fourier-like equation. The latter equation, in fact, predicts a completely flat profile whereas we have, instead, a flat profile except for a very narrow zone near the walls, where there is a steep increase of the heat-flux profile from a low value to the flat value. This mathematical discrepancy is not a truly physical discrepancy, because in strict terms the

Fourier law is only valid for special scales larger than the phonon mean-free path. Thus, since for small values of Kn the phonon mean-free path is much smaller than the width of the strip, the discrepancy is not only quantitatively negligible in reference to the total heat flux, but it is also conceptually admissible because it is found out of the range of validity of Fourier law. Anyway, it is an interesting question which should be explored in deeper detail in computer simulations. In fact, such a steep increase of the heat flow near the walls has been modeled on other grounds than here (i.e., without incorporating the Laplacian term in Eq. (1)) by assuming that the thermal resistance is higher than that predicted by Fourier law near the walls, in a factor $[1 - \exp(-D/\ell)]^{-1}$, D being the diameter of the channel [43, 44]. The subtle details of this simplified, but efficient, model and our model should be considered in a deeper way.

2. Moderate values of Kn *(Poiseuille phonon flow)*

For moderate values of the Knudsen number, the heat-transfer regime is in transition from the diffusive regime to the ballistic one. In particular, for increasing values of Kn (i.e., whenever ℓ becomes comparable to, or larger than, the width w of the strip), the phonon bulk scattering gradually reduces, and the phonon-wall scattering increases. Moreover, the phonons show a macroscopic drift motion. In this case, the boundary-phonon scattering becomes prevalent among the other scattering mechanisms. The heat flux is smaller near the walls because the boundary-phonon scattering is mainly felt in their neighborhood. This explains the parabolic profile of the local heat flux we can see, for example, in Fig. 2 when $\mathrm{Kn} = 0.1$, $\mathrm{Kn} = 0.5$ and $\mathrm{Kn} = 1$. Since in this case the higher Kn, the smaller the maximum value of q, then we may infer that phonon-boundary collisions are the main mechanism of momentum loss and resistance to the heat flow, especially for small values of C_1 (i.e., for diffusive phonon-wall collisions predominating over specular ones). Instead, for higher values of C_1, the parabolic profile is not so evident, as the slip flow makes them closer to a flat profile.

3. Large values of Kn *(ballistic regime)*

When Kn gets large values (for example when Kn ≈ 10 in the case of study of the present paper), the regime of heat transfer becomes ballistic. In this regime the phonons suffer only scant internal (i.e., in the bulk of the system) scattering. As it can be seen from Fig. 2, in this case the heat flux attains again a uniform profile, similar to that observed in diffusive regime. In particular, if Kn $\to \infty$, the heat-flux profile tends to the following (ballistic) limit behavior

$$q_{\mathrm{ball,lim}} = \lambda C_1 \tanh\left(\frac{1}{2\,\mathrm{Kn}}\right)\frac{\Delta T}{L} \approx \lambda\left(\frac{C_1}{2\,\mathrm{Kn}}\right)\frac{\Delta T}{L}. \tag{11}$$

It seems worth noticing that in contrast to the flat heat-flux profile we recover for very low values of the Knudsen number (i.e., when Eq. (10) holds), the flat heat-flux profile arising from Eq. (11) depends both on the width of the strip, for a given ℓ (i.e., for a given temperature) through the Knudsen number, and on C_1 as it is logical to expect.

From the physical point of view, Eq. (11) can be explained in the following way. When Kn reaches high enough values, the Knudsen layer pervades the main part of the cross section. In this case, the frequency of phonon-boundary interactions is so high that phonon-boundary scattering is the main event, and the consequent reduction of the local heat-flux amplitude due to the momentum loss becomes again homogeneous in the whole transversal section. It seems worth observing that in Refs. [1, 34, 35] the authors draw the same conclusion, but with an alternative way of accounting for the boundary conditions (namely, by using Eq. (2) instead of Eq. (3)). Let us also observe that the higher C_1, the smaller the values of Kn at which this second limit behavior occurs.

As interpreted from the point of view of the width w the three regime mentioned above are as follows: diffusive (Fourier transport) is found for $w > \ell_R$, with ℓ_R the mean-free path of resistive collisions, the Poiseuille phonon flow for $\ell_N < w < \ell_R$, with ℓ_N the mean-free path of normal collisions, and the ballistic flow for $w < \ell_N, \ell_R$.

B. Results for the effective thermal conductivity

The effective thermal conductivity (ETC) of narrow strips is much reduced with respect to that of wide strips of the same material [6]. Since the thermal conductivity of solid

thin layers is important for the design of field-effect transistors in electronic circuits, coated lenses in laser systems, and microfabricated superconducting radiation detectors [20, 21], then theoretical model predicting it may be useful in practical applications.

Starting from the results obtained in Sec. II A, here we derive a theoretical model for the ETC in thin layers, defined as

$$\lambda_{\text{eff}} \equiv \left(\frac{Q_{\text{tot}}}{A}\right) \frac{L}{\Delta T} = \left[\frac{1}{w} \int_{-0.5}^{+0.5} q\left(y_*\right) dy_*\right] \frac{L}{\Delta T}, \tag{12}$$

where A is the area of its cross section, and Q_{tot} is the total heat per unit of time flowing in the system. Indeed, in the 2D case, instead of a cross section A, only the width w must be used in the denominator of Eq. (12).

Combining Eqs. (9) and (12) one is lead to the following expression for the ETC in narrow strips (or very thin layers):

$$\lambda_{\text{eff}}\left(\text{Kn}\right) = \lambda \left[1 - \frac{2\,\text{Kn}\tanh\left(\frac{1}{2\,\text{Kn}}\right)}{1 + C_1 \tanh\left(\frac{1}{2\,\text{Kn}}\right)}\right]. \tag{13}$$

The theoretical prediction in Eq. (13) differs from the expression

$$\lambda_{\text{eff}}\left(\text{Kn}\right) = \lambda \left\{1 - 2\,\text{Kn}\tanh\left(\frac{1}{2\,\text{Kn}}\right)\left[1 - C_1 \tanh\left(\frac{1}{2\,\text{Kn}}\right)\right]\right\}, \tag{14}$$

obtained in Ref. [35]. The discrepancy between Eq. (13) and Eq. (14) is due to the different way the boundary conditions have been used to study the thermal transport in nanosystems (namely, in the form of Eq. (3) for the theoretical model (13), and in the form of Eq. (2) for the theoretical model (14)). However, for large values of Kn, Eqs. (13) and (14) predict that the ETC behaves as

$$\lambda_{\text{eff,ball}}\left(\text{Kn}\right) = \lambda \left(\frac{C_1}{2\,\text{Kn}}\right), \tag{15}$$

in agreement with the experimental observations showing that the ETC in nanosystems decreases as Kn^{-1} for increasing Knudsen number in the ballistic regime [1, 2, 35], i.e., when $\text{Kn} \gg 1$. Similarly, for very low values of Kn (i.e., in the Fourier diffusive regime), both Eq. (13) and (14) turn out $\lambda_{\text{eff}} = \lambda_{\text{eff,diff}} \equiv \lambda$.

By means of Eq. (13), in Fig. 3 we plot the behavior of the nondimensional ETC $\lambda_* = \lambda_{\text{eff}}/\lambda$ in a 2D strip as a function of the Knudsen number $\text{Kn} = \ell/w$ for different values of the nondimensional product $C_1 \equiv a\left(T\right) C$ (i.e., $C_1 = 0.05$, $C_1 = 0.5$, $C_1 = 2$ and $C_1 = 10$) accounting for the diffusive and specular phonon-wall interactions.

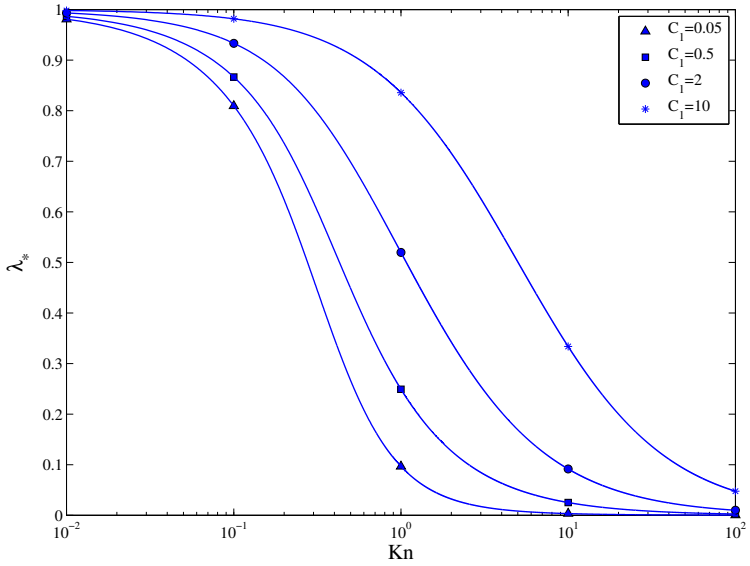

FIG. 3: Nondimensional ETC $\lambda_* = \lambda_{\text{eff}}/\lambda$ versus the Knudsen number for different values of the nondimensional product $C_1 \equiv a\,(T)\,C$: theoretical behavior arising from Eq. (13). In figure the x axis is in a logarithmic length scale.

As it can be seen from Fig. 3, in the ballistic regime (i.e., when $\text{Kn} \gg 1$) the ETC is much reduced with respect to that characterizing the diffusive regime (i.e., when $\text{Kn} \ll 1$).

III. COMPARISON WITH THE GUYER-KRUMHANSL FORMALISM

Though we previously referred to Eq. (1) as the Guyer-Krumhansl (GK) equation, it has in fact important differences with respect to the original proposal of those authors [23, 24], especially regarding the way as the phonon-wall collisions are included in the model. In the approach used in Sec. II (as well as in that of Refs. [1, 35]), in the differential equation (1) it has been used the usual bulk thermal conductivity obtained as the usual Ziman limit [47], that is, $\lambda = c_v \overline{\text{v}}^2 \tau_{R0}/3$, wherein c_v is the specific heat at constant volume per unit volume, $\overline{\text{v}}$ the average phonon speed and τ_{R0} the characteristic time of resistive phonon collisions in the bulk, given by

$$\tau_{R0}^{-1} = \tau_{\text{u}}^{-1} + \tau_{\text{i}}^{-1} + \tau_{\text{d}}^{-1}, \tag{16}$$

being τ_{u} the relaxation time of umklapp phonon-phonon collisions, τ_{i} the relaxation time of phonon-impurity collisions, and τ_{d} the relaxation time of phonon-defect collisions. The

phonon-wall interactions have been then accounted for suitable boundary conditions [1, 29, 35], which in the present case are given by Eq. (3).

Indeed, in Ref. [24] the authors considered a boundary relaxation-time τ_{b} that they combined with the usual relaxation time τ_{R0} due to bulk resistive mechanisms by means of Matthiessen rule as

$$\tau_R^{-1} = \tau_{\mathrm{u}}^{-1} + \tau_{\mathrm{i}}^{-1} + \tau_{\mathrm{d}}^{-1} + \tau_{\mathrm{b}}^{-1} \equiv \tau_{R0}^{-1} + \tau_{\mathrm{b}}^{-1}, \tag{17}$$

with $\tau_{\mathrm{b}} = wb\left(T\right)/\overline{\mathrm{v}}$, with $b\left(T\right)$ being a suitable nondimensional temperature function depending on the form of the cross section of the system and on the relative abundance of specular and diffusive phonon-wall collisions.

Once the combined resistive-boundary (phonon-wall) collision time has been obtained, the thermal conductivity λ_{GK} (depending on the size of the system through τ_{b}) was calculated, and used in the first term of the right-hand side of Eq. (1). In particular, it is obtained

$$\lambda_{\mathrm{GK}} = \frac{1}{3} c_v \overline{\mathrm{v}}^2 \left(\frac{\tau_{R0}\tau_{\mathrm{b}}}{\tau_{R0} + \tau_{\mathrm{b}}} \right) = \lambda \left(1 + \frac{\tau_{R0}}{\tau_{\mathrm{b}}} \right)^{-1} = \lambda \left[1 + b\left(T\right) \frac{\ell}{w} \right]^{-1} = \frac{\lambda}{1 + b\left(T\right) \mathrm{Kn}}, \tag{18}$$

wherein $\ell = \tau_{R0}\overline{\mathrm{v}}$. To this contribution one adds, in some regime, the hydrodynamic contribution due to the normal (momentum-conserving) phonon-phonon collisions, which is described by the non-local term in the right-hand side of Eq. (1) and whose microscopic effects have been explored in much detail in Refs. [14, 15].

It is also important to note that in Eq. (1) ℓ means the average phonon mean-free path obtained from the Ziman expression for the bulk thermal conductivity, i.e., $\ell = \lambda \left[\left(1/3\right) c_v \overline{\mathrm{v}} \right]^{-1} \equiv \overline{\mathrm{v}}\tau_{R0}$, whereas in the original version of the GK equation one has, instead of $a^2\ell^2$, $\ell_{\mathrm{GK}}^2 = \overline{\mathrm{v}}^2 \tau_N \tau_R / 5$, where τ_N is the characteristic collision time of normal (momentum conserving), phonon-phonon collisions. In terms of $a^2\ell^2$, the coefficient a^2 could be obtained by equating $a^2\ell^2 = \ell_{\mathrm{GK}}^2$, namely, $a^2\left(T\right) = \tau_N\left(T\right)/5\tau_R\left(T\right)$.

A further observation is that in GK approach, the non-slip boundary condition for $\mathbf{q}$ is considered, namely, $\mathbf{q}|_\gamma = 0$, and the effects of the boundary collisions are considered in the form (18) of the ETC. The term in $\nabla^2\mathbf{q}$ is supposed to describe only an additional contribution of the walls restricted to the case when phonon display a collective behaviors when normal collisions are dominating with respect to resistive ones [14, 15].

This alternative approach, in steady states, yields the following behavior for the local

heat flux across any cross section of the strip:

$$q\left(y\right)=\frac{\lambda}{1+2b\,\mathrm{Kn}}\left[1-\frac{\cosh\left(\frac{y}{a\ell}\right)}{\cosh\left(\frac{1}{2a\,\mathrm{Kn}}\right)}\right]\frac{\Delta T}{L}. \tag{19}$$

When $a\to 0$, Eq. (19) becomes a flat heat profile

$$q\left(y\right)=\left(\frac{\lambda}{1+2b\,\mathrm{Kn}}\right)\frac{\Delta T}{L}. \tag{20}$$

For small Kn this is the Fourier's result in Eq. (10), whereas for high Kn it is analogous to Eq. (11) if $b\left(T\right)$ is identified as $b\left(T\right)=\left[a\left(T\right)C\right]^{-1}$ (for a different geometry, the relation between $b\left(T\right)$ and $a\left(T\right)C$ would also have a form-dependent numerical factor). When $a\to\infty$, instead, Eq. (19) tends to the Poiseuille profile

$$q\left(y\right)=\left(\frac{\lambda}{1+2b\,\mathrm{Kn}}\right)\left(\frac{1}{2\ell^{2}}\right)\left[\left(\frac{w}{2}\right)^{2}-y^{2}\right]\frac{\Delta T}{L}. \tag{21}$$

Finally, by the definition of ETC in Eq. (12) in this case we have

$$\lambda_{\mathrm{eff}}\left(\mathrm{Kn}\right)=\frac{\lambda}{1+2b\,\mathrm{Kn}}\left[1-2a\,\mathrm{Kn}\tanh\left(\frac{1}{2a\,\mathrm{Kn}}\right)\right]. \tag{22}$$

In Fig. 4 we compare the results arising from our phonon-hydrodynamic approach with those arising from the GK formalism. The comparison involves both the heat-flux profile (upper subplot in figure), and the ETC (lower subplot in figure). To compare the heat-flux profile we used Eqs. (9) and (19) in the case of $\mathrm{Kn}=0.2$. To compare the ETC we used, instead, Eq. (13) and Eq. (22). For the sake of computation, we assumed $a=1$, $C=5$, and $b=C^{-1}\equiv 0.2$.

As it can be seen from Fig. 4, both for q_{*}, and for λ_{*} the phonon-hydrodynamic approach predicts larger values than the GK formalism.

In closing the present section it is important to stress that both the theoretical heat-flux profile in Eq. (9), and the theoretical ETC in Eq. (13) are strictly related to the non-dimensional parameter $a\left(T\right)$ and C. Although in Refs. [1, 8, 34], for example, deeper investigations on their physical interpretations can be found, the very important role those parameters play requires further studies. To this end, it would be useful to infer information about them from the comparison of our theoretical model with other existing models, experimental data or simulation results.

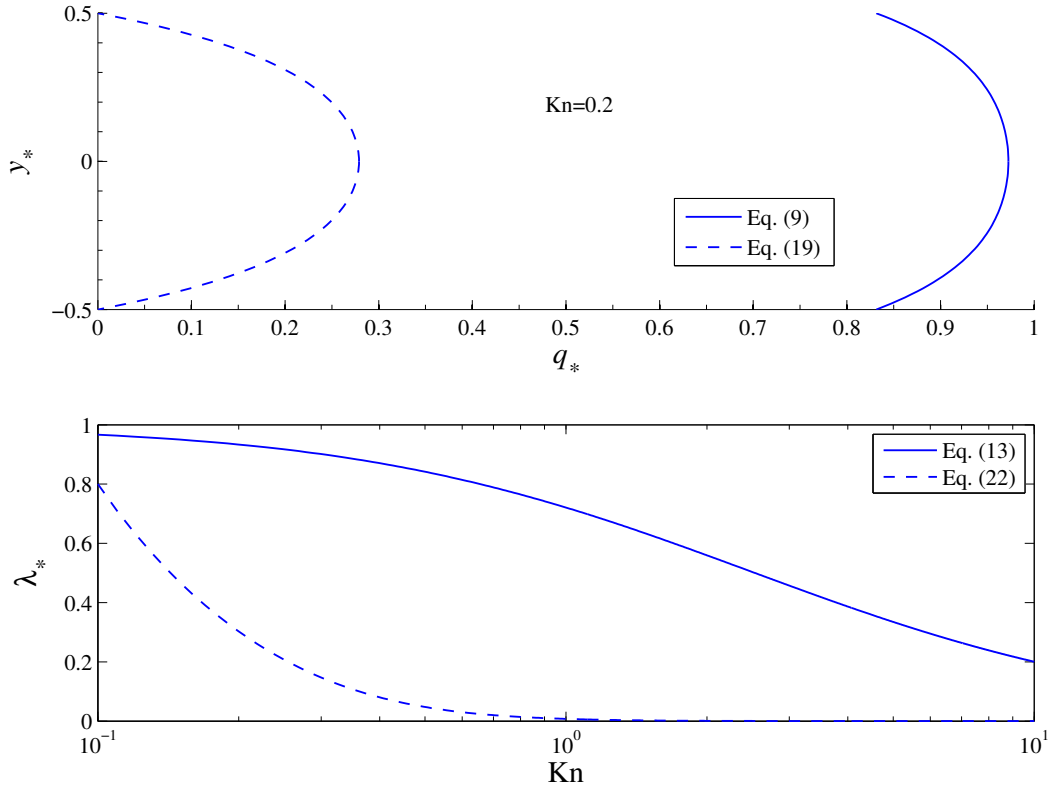

FIG. 4: Phonon-hydrodynamic approach versus GK formalism: qualitative comparison. In the upper subplot the nondimensional heat-flux profiles $q_* = q/(\Delta T/L)$ across the strip arising from Eqs. (9) and (19) when Kn = 0.2 are compared. In the lower subplot, instead, as a function of Kn we compare the nondimensional ETC $\lambda_* = \lambda_{\rm eff}/\lambda$ arising from Eq. (13) with that arising from Eq. (22). In this subfigure the x axis is in a logarithmic length scale.

IV. CONCLUSIONS

In the present paper we have examined the heat-flux profile across a narrow 2D strip as a function of the Knudsen number $\mathrm{Kn} \equiv \ell/w$ using two different forms of a generalized heat-transport equation containing second-order non-local terms. From the model based on Eqs. (1)-(3), we have found that the heat-flux profile in a generic transversal section is given by Eqs. (9). In particular, that profile has a flat shape given by Eq. (10) for $\mathrm{Kn} \ll 1$ (i.e., in the Fourier regime), a parabolic one at intermediate Kn (between 0.1 and 1, for instance, depending on the values of the slip coefficient C), and again a practically flat profile as in Eq. (11) for high Kn (i.e., in the ballistic regime). Thus, the Poiseuille flow with a parabolic

profile is found only in a given temperature range, or a given size range for the strip width.

In the original Guyer-Krumhansl model based on Eqs. (1) and (18), the parabolic heat profile is also found in some restricted temperature (or size) range. Conceptually, both formalisms of non-local heat transport agree on this specific range for hydrodynamic phonon flow.

The most interesting difference between both models rests on the boundary conditions used for $\mathbf{q}$ on the walls, and on the way of accounting for the phonon-wall collisions. In the model based on Eqs. (1) and (3), the nonvanishing boundary conditions imply a slip heat flow along the walls, whereas in the model based on Eqs. (1) and (18) non-slip conditions are imposed on the heat flux. Furthermore, in the approach based on Eqs. (1) and (18), the size-dependent thermal conductivity (18) describes the phonon-wall collisions, whereas in the description based on Eqs. (1) and (3) the role of the shape of the system is more explicit (through the use of Eq. (3), and of the relative role of specular or diffusive collisions). In this case, the presence of a slip flow also connects in a smooth way the hydrodynamic phonon regime to the ballistic regime.

In summary, a possible way of checking how phonon-wall effects should be more faithfully included into a generalized heat-transport equation with non-local terms, would be to check whether the heat flux exhibits some slip effects along the walls, especially in strip of suspended graphene, where the hydrodynamic regime is expected to show at a relatively wide range of temperatures around 100 K, in contrast to bulk materials, were it is shown at low temperatures (1 K −2 K) in a narrow temperature range [30]. If there is such a slip flow, the dependence of the effective thermal conductivity on the width w of the layer would not be on w^2, as in Poiseuille flow analogy, but slightly different because of the profile would be slightly flatter. This would not mean, however, that collective hydrodynamic effects are not present, but that their manifestation is somewhat obscured by the effects of the slip flux.

At the very end, it seems wort noticing that here we have considered narrow but long strips, in such a way that only boundary effects on the lateral walls have been taken into account. In the case of short strips, instead, the effects on the entrance and exit boundaries have to be also taken into account. The physical mechanism for these boundary effects is different from that on the lateral walls [17, 25], as it is manifested, for instance, in the anisotropy in-plane and cross-plane thermal conductivity in narrow films [17]. Therefore, in the future it would be interesting to consider both this aspect, and the so-called *entrance*

effects which are found in the hydrodynamic analyses of short channels.

Data Accessibility statement

The nondimensional heat flux $q_* = q/\left(\Delta T/L\right)$ and the nondimensional effective thermal conductivity $\lambda_* = \lambda_{\text{eff}}/\lambda$ we plotted in Figs. 2–4 allowed us to avoid the use of experimental data. All the results of the present article are fully reproducible by means of the data we provided above.

Competing interests statement

All authors have no competing interests.

Authors' contributions statement

All authors gave the same contribution.

Funding statement

A. S. acknowledges the financial support of the Italian Gruppo Nazionale per la Fisica Matematica (GNFM-INdAM). I.C. acknowledges the financial support from the University of Basilicata and from the University of Salento for her stay in the Autonomous University of Barcelona as part of her doctoral studies. D. J. acknowledges the financial support of the Spanish Ministry of Economy and Competitiveness under grant FIS 2012-33099, and the Ministry of Science and Innovation under the Consolider Project Nano Therm (grant CSD-2010-00044).

---

[1] Alvarez, F. X., Jou, D., and Sellitto, A. (2009) Phonon hydrodynamics and phonon-boundary scattering in nanosystems. *J. Appl. Phys.*, **105**, 014317 (5 pages). doi:http://dx.doi.org/10.1063/1.3056136

[2] Asheghi, M., Leung, Y. K., Wong, S. S., and Goodson, K. E. (1997) Phonon-boundary scattering in thin silicon layers. *Appl. Phys. Lett.*, **71**, 1798–1800. doi:http://dx.doi.org/10.1063/1.119402

[3] Balandin, A. A. (2011) Thermal properties of graphene and nanostructured carbon materials. *Nat. Mater.*, **10**, 569–581. doi:10.1038/nmat3064

[4] Balandin, A. A., Ghosh, S., Baoand, W., Calizo, I., Teweldebrhan, D., Miao, F., and Lau, C.-N. (2008) Superior thermal conductivity of single-layer graphene. *Nano Lett.*, **8**, 902–907. doi:10.1021/nl0731872

[5] Bernini, U., Lettieri, S., Maddalena, P., Vitiello, R., and Di Francia, G. (2001) Evaluation of the thermal conductivity of porous silicon layers by an optical pump-probe method. *J.Phys.: Condens. Matter*, **13**, 1141–1150. doi:10.1088/0953-8984/13/5/327

[6] Cahill, D. C., Fischer, H. E., Klitsner, T., O., E. T. S. R., and Pohl (1989) Thermal Conductivity of Thin Films: Measurements and Understanding. *J. Vac. Sci. Technol.*, **A7**, 1259–1266. doi:http://dx.doi.org/10.1116/1.576265

[7] Cahill, D. G., et al. (2014) Nanoscale thermal transport. II. 2003-2012. *Appl. Phys. Rev.*, **1**, 011305 (45 pages). doi:http://dx.doi.org/10.1063/1.4832615

[8] Carlomagno, I., Sellitto, A., and Jou, D. (2015) Effective phonon mean-free path and slip heat flow in rarefied phonon hydrodynamics. *Phys. Lett. A*, In Press - Corrected Proof. doi:10.1016/j.physleta.2015.05.044

[9] Cepellotti, A., Fugallo, G., Paulatto, L., Lazzeri, M., Mauri, F., and Marzari, N. (2015) Phonon hydrodynamics in two-dimensional materials. *Nature Comm.*, **6**, 6400 (7 pages). doi:10.1038/ncomms7400

[10] Cercignani, C. (2006) *Slow Rarefied Flows - Theory and Application to Micro-Electro-Mechanical Systems*. Birkhäuser Verlag, Basel.

[11] Chen, G. (2001) Ballistic-Diffusion Equations for Transient Heat Conduction From Nano to Macroscales. *J. Heat Transfer - T. ASME*, **124**, 320–328. doi:10.1115/1.1447938

[12] Cimmelli, V. A. (2009) Different thermodynamic theories and different heat conduction laws. *J. Non-Equilib. Thermodyn.*, **34**, 299–333. doi:10.1515/JNETDY.2009.016

[13] Cimmelli, V. A., Sellitto, A., and Jou, D. (2010) Nonequilibrium temperatures, heat waves, and nonlinear heat transport equations. *Phys. Rev. B*, **81**, 054301 (9 pages). doi:http://dx.doi.org/10.1103/PhysRevB.81.054301

[14] De Tomas, C., Cantarero, A., Lopeandia, A. F., and Alvarez, F. X. (2014) From kinetic to collective behavior in thermal transport on semiconductors and semiconductor nanostructures. *J. Appl. Phys.*, **115**, 164314. doi:http://dx.doi.org/10.1063/1.4871672

[15] De Tomas, C., Cantarero, A., Lopeandia, A. F., and Alvarez, F. X. (2014) Thermal conductivity of group-IV Semiconductors from a Kinetic-Collective Model. *Proc R. Soc. A*, **470**, 20140371 (12 pages). doi:10.1098/rspa.2014.0371

[16] Dong, Y., Cao, B.-Y., and Guo, Z.-Y. (2011) Generalized heat conduction laws based on thermomass theory and phonon hydrodynamics. *J. Appl. Phys.*, **110**, 063504 (6 pages). doi:10.1063/1.3634113

[17] Dong, Y., Cao, B.-Y., and Guo, Z.-Y. (2015) Ballistic-diffusive phonon transport and size induced anisotropy of thermal conductivity of silicon nanofilms. *Physica E*, **66**, 1–6. doi:10.1016/j.physe.2014.09.011

[18] Geim, A. K. and Novoselov, K. S. (2007) The rise of graphene. *Nat. Mater.*, **6**, 183–191. doi:10.1038/nmat1849

[19] Gombosi, T. I. (1994) *Gaskinetic Theory*. Cambridge University Press, Cambridge.

[20] Goodson, K. E. and Flik, M. I. (1992) Effect of Microscale Thermal Conduction on the Packing limit of Silicon-on-Insulator Electronic Devices. *IEEE Trans. Components, Hybrids, and Manufacturing Technology*, **15**, 715–722. doi:10.1109/33.180035

[21] Goodson, K. E. and Flik, M. I. (1994) Solid Layer Thermal-Conductivity Measurement Techniques. *Appl. Mech. Rev.*, **47**, 101–112. doi:10.1115/1.3111073

[22] Grmela, M., Lebon, G., Dauby, P. C., and Bousmina, M. (2005) Ballistic-diffusive heat conduction at nanoscale: GENERIC approach. *Phys. Lett. A*, **339**, 237–245. doi:10.1016/j.physleta.2005.03.048

[23] Guyer, R. A. and Krumhansl, J. A. (1966) Solution of the linearized phonon Boltzmann equation. *Phys. Rev.*, **148**, 766–778. doi:http://dx.doi.org/10.1103/PhysRev.148.766

[24] Guyer, R. A. and Krumhansl, J. A. (1966) Thermal conductivity, second sound and phonon hydrodynamic phenomena in nonmetallic crystals. *Phys. Rev.*, **148**, 778–788. doi:http://dx.doi.org/10.1103/PhysRev.148.778

[25] Hua, Y.-C. and Cao, B.-Y. (2014) Phonon ballistic-diffusive heat conduction in silicon nanofilms by Monte Carlo simulations. *Int. J. Heat Mass Transfer*, **78**, 755–759. doi:10.1016/j.ijheatmasstransfer.2014.07.037

[26] Jou, D., Casas-Vázquez, J., and Lebon, G. (2010) *Extended Irreversible Thermodynamics*. Springer, Berlin, fourth revised edn.

[27] Kovács, R. and Ván, P. (2015) Generalized heat conduction in heat pulse experiments. *Int. J. Heat Mass Transfer*, **83**, 613–620. doi:10.1016/j.ijheatmasstransfer.2014.12.045

[28] Lebon, G. (2014) Heat conduction at micro and nanoscales: A review through the prism of Extended Irreversible Thermodynamics. *J. Non-Equilib. Thermodyn.*, **39**, 35–59. doi:10.1515/jnetdy-2013-0029

[29] Lebon, G., Machrafi, H., Grmela, M., and Dubois, C. (2011) An extended thermodynamic model of transient heat conduction at sub-continuum scales. *Proc. R. Soc. A*, **467**, 3241–3256. doi:10.1098/rspa.2011.0087

[30] Lee, S., Broido, D., Esfarjani, K., and Chen, G. (2015) Hydrodynamic phonon transport in suspended graphene. *Nature Comm.*, **6**, 6290 (9 pages). doi:10.1038/ncomms7290

[31] Li, D., Wu, Y., Kim, P., Shi, L., Yang, P., and Majumdar, A. (2003) Thermal conductivity of individual silicon nanowires. *Appl. Phys. Lett.*, **83**, 2934–2936. doi:http://dx.doi.org/10.1063/1.1616981

[32] Liu, W. and Asheghi, M. (2004) Phonon-boundary scattering in ultrathin single-crystal silicon layers. *Appl. Phys. Lett.*, **84**, 3819–3821. doi:http://dx.doi.org/10.1063/1.1741039

[33] Ma, Y. (2012) Size-dependent thermal conductivity in nanosystems based on non-Fourier heat transfer. *Appl. Phys. Lett.*, **101**, 211905 (5 pages). doi:http://dx.doi.org/10.1063/1.4767337

[34] Sellitto, A., Alvarez, F. X., and Jou, D. (2010) Second law of thermodynamics and phonon-boundary conditions in nanowires. *J. Appl. Phys.*, **107**, 064302 (7 pages). doi:http://dx.doi.org/10.1063/1.3309477

[35] Sellitto, A., Alvarez, F. X., and Jou, D. (2012) Geometrical dependence of thermal conductivity in elliptical and rectangular nanowires. *Int. J. Heat Mass Transfer*, **55**, 3114–3120. doi:10.1016/j.ijheatmasstransfer.2012.02.045

[36] Struchtrup, H. (2005) *Macroscopic transport equations for rarefied gas flows: approximation methods in kinetic theory - Interaction of Mechanics and Mathematics*. Springer, Heidelberg.

[37] Tzou, D. Y. (2011) Nonlocal behavior in phonon transport. *Int. J. Heat Mass Transfer*, **54**, 475–481. doi:10.1016/j.ijheatmasstransfer.2010.09.022

[38] Tzou, D. Y. (2014) *Macro- to Microscale Heat Transfer: The Lagging Behaviour*. Wiley, United Kingdom, second edn.

[39] Tzou, D. Y. and Guo, Z.-Y. (2010) Nonlocal behavior in thermal lagging. *Int. J. Thermal Sci.*, **49**, 1133–1137. doi:10.1016/j.ijthermalsci.2010.01.022

[40] Usenko, A. Y., Carr, W. N., and Chen, B. (2004) Transfer of single crystalline silicon nanolayer onto alien substrate. *Nanotechnology*, **3**, 225–229. doi:10.1109/TNANO.2004.828519

[41] Ván, P. and Fülöp, T. (2012) Universality in heat conduction theory: weakly nonlocal thermodynamics. *Ann. Phys.*, **524**, 470–478. doi:10.1002/andp.201200042

[42] Wang, M., Cao, B.-Y., and Guo, Z.-Y. (2010) General heat conduction equations based on the thermomass theory. *Frontiers Heat Mass Transfer*, **1**, 013004 (8 pages). doi:http://dx.doi.org/10.5098/hmt.v1.1.3004

[43] Wang, M., and Guo, Z.-Y. (2010) Understanding of temperature and size dependences of effective thermal conductivity of nanotubes. *Phys. Lett. A*, **374**, 4312–4315. doi:10.1016/j.physleta.2010.08.058

[44] Wang, M., Yang, N., and Guo, Z.-Y. (2011) Non-Fourier heat conductions in nanomaterials. *J. Appl. Phys.*, **110**, 064310 (7 pages). doi:10.1063/1.3634078

[45] Xu, M. (2014) Slip boundary condition of heat flux in Knudsen layers. *Proc. R. Soc. A*, **470**, 20130578 (9 pages). doi:10.1098/rspa.2013.0578

[46] Zhang, Z. M. (2007) *Nano/Microscale Heat Transfer*. McGraw-Hill, New York.

[47] Ziman, J. M. (2001) *Electrons and Phonons*. Oxford University Press, Oxford.